Crash reconstruction technique for cable barrier systems

Mojdeh Asadollahi Pajouh, Jennifer D. Schmidt, Curt L. Meyer, Karla A. Lechtenberg & Ronald K. Faller

Taylor & Francis
Taylor & Francis Group

Check for updates

Crash reconstruction technique for cable barrier systems

Mojdeh Asadollahi Pajouh [iD][a], Jennifer D. Schmidt[b], Curt L. Meyer[c],
Karla A. Lechtenberg[b], and Ronald K. Faller[b]

[a]Civil Engineering, Midwest Roadside Safety Facility, University of Nebraska–Lincoln, Lincoln, Nebraska, USA; [b]Midwest Roadside Safety Facility, University of Nebraska–Lincoln, Lincoln, Nebraska, USA; [c]Bates Technical College, Tacoma, Washington, USA

ABSTRACT

Cable barrier systems consisting of steel cables mounted on widely spaced weak posts are one of the most commonly used guardrail systems to protect errant vehicles from roadside hazards. When a vehicle impacts cable barriers, the cables are stretched, producing tension forces that safely redirect the impacting vehicle. The estimation of the energy absorbed during a vehicle barrier crash can aid in accident reconstructions, as it relates to estimation of the initial impact velocity, crash severity, and other accident features such as the occupant injuries during the accident. This article details an accident reconstruction technique developed for estimating the energy absorbed during a cable barrier impact. This absorbed energy comprises several components: (1) plastic deformation and rotation of posts in soil or a rigid foundation, (2) tire-ground interaction, (3) internal cable energy, and (4) frictional losses during vehicle-barrier interaction. Charts were developed to estimate the energy absorbed by deforming S3 × 5.7 posts. Three full-scale crash tests, conducted on straight and curved, three-cable barrier systems were used to validate the proposed methods. For both systems, the vehicles' estimated initial velocities using the reconstruction technique were within 1% and 10% of the actual velocities of the vehicle, respectively.

1. Introduction

Accident reconstruction is a crucial step to evaluate crash severity. It involves estimating the energy absorbed during a crash as well as initial vehicle velocity. Accident reconstruction techniques utilize fundamental concepts including conservation of energy and conservation of momentum as well as the available information to determine how the accident occurred. Several reconstruction procedures have been developed for various roadside safety devices such as longitudinal W-beam guardrail barriers, breakaway poles, and luminaries. In 1990, Mak,

Sicking and Lock developed reconstruction procedures for rigid barrier impacts. In this study, a new subroutine was introduced for the software package CRASH3 to analyze the vehicle trajectory and estimate the initial energy lost in a rigid barrier impact based on vehicle crush and the contact length of the vehicle on the barrier. The original impact velocity was then determined through conservation of energy. Curves were developed to estimate vehicle speed from the travelled distance. Coon and Reid (2005) reported a reconstruction technique for longitudinal barrier crashes. The method incorporated the principle of energy conservation. The energy losses through means such as vehicle crush, rail deformation, post deformation, vehicle-ground friction, and vehicle-barrier friction were estimated through simulations using BARRIER VII software (Powell, 1973). The initial kinetic energy and velocity were approximated by adding the energy losses during the impact with the barrier to the vehicle's kinetic energy when it departed the barrier. The reconstruction procedure developed was compared to full-scale crash tests and estimated impact velocities were within 3%. Coon and Reid (2006) also developed a method to reconstruct vehicle impacts into energy-absorbing guardrail end terminals derived from full-scale crash tests results. For analysis of the initial portion of the impact, where the terminal head and the vehicle reach the same velocity, conservation of momentum was applied, and then the energy absorbed by the end terminal was added to kinetic energy when the vehicle departed the system to determine the initial kinetic energy.

Low-tension cable barrier systems are one of the most commonly used longitudinal guardrail systems to protect vehicles from roadside hazards. Despite its prevalence, there is no method for reconstructing cable barrier impacts. As an errant vehicle penetrates into the cable barrier upon impact, the posts deflect and the cables are stretched producing tension forces that redirect the vehicle back toward the roadway. The deflection of the system and energy absorbed throughout the impact event limits the accelerations applied to the occupants of the impacting vehicle. Further, cable tension diminishes as an impacting vehicle begins to exit the system, thereby minimizing the risk of the vehicle being projected back into traffic in an uncontrolled manner. The kinetic energy of a vehicle decreases in a run-off-road crash through rolling resistance, braking, sliding, deformation, or fracture of impacted objects, friction, and other factors. Quantifying the energy absorbed through each of these events can help reconstruct the initial velocity of the vehicle through the principle of conservation of energy. However, determining if or when these events happened and the amount of energy absorbed through each event can be difficult to quantify. Therefore, a reconstruction procedure was developed to estimate the vehicle initial velocity and the energy absorbed during a vehicular impact with a cable barrier system. Recommendations for improving the predictive reconstruction procedure are also presented. Three full-scale crash tests, conducted on straight and curved, low-tension, three-cable barrier systems were used to validate the proposed methods (Schmidt, Lechtenberg, et al., 2013; Terpsma et al., 2008).

2. Description of full-scale crash tests

2.1. Straight cable barrier system: Test No. CS-2

A 150.6-m (494-ft) long, low-tension, three-cable barrier system was evaluated according to National Cooperative Research Program (NCHRP) Report 350 safety performance criteria (Ross, Sicking, Zimmer, & Michie, 1993). Three 19-mm ($^3/_4$-in.) diameter cables comprising 3 × 7 wire rope with an upper-most mounting height of 762 mm (30 in.) and with 76-mm (3-in.) incremental spacing for the two lower cables were supported by ninety-two S3 × 5.7 steel guardrail posts spaced at 1,219 mm (4 ft), as shown in Figure 1. The ends of the cables were threaded rods that terminated in a cable anchor. The posts were installed 1,219 mm (4 ft) behind the slope breakpoint of a 1.5 H:1 V sloped ditch.

In Test No. CS-2, the three-cable barrier system was impacted by a 2,033-kg (4,481-lb) pickup truck at a speed of 99.1 km/h (61.6 mph) and at an angle of 25 degrees (Terpsma et al., 2008). The barrier adequately contained and redirected the vehicle with controlled lateral displacements of the barrier system. The maximum lateral dynamic cable deflection was 3,163 mm (124.5 in.), as determined from high-speed digital video analysis. The test met the safety performance criteria of NCHRP Report 350 (Ross et al., 1993). The velocity of the pickup truck was approximately 52.8 km/h (32.8 mph) when the vehicle exited the system. The impact conditions are summarized in Table 1.

**Figure 1.** Test installation: straight cable barrier system.

Table 1. Full-scale crash tests on low-tension, three-cable barrier systems.

Test No.	Cable Barrier System	Test Vehicle	Impact Conditions	
			Speed (km/h)	Angle (deg)
CS-2	Straight	2,033-kg pickup truck	99.1	25
NYCC-1	Exterior-Curved	2,277-kg pickup truck	99.1	19.9
NYCC-3	Exterior-Curved	2,267-kg pickup truck	101.6	21.6

2.2. Exterior-curved cable barrier system: Test Nos. NYCC-1 and NYCC-3

In Test No. NYCC-1, a 121.9-m (400-ft) long, three-cable, exterior-curved cable barrier system with a radius of 109.7 m (360 ft), as shown in Figure 2a, was evaluated according to the *Manual for Assessing Safety Hardware (MASH)* safety performance criteria (AASHTO, 2009) for modified test designation no. 3–11. Three 19-mm ($^3/_4$-in) diameter 3 × 7, Class A galvanized wire ropes were supported by forty S3 × 5.7 steel guardrail posts. The cables were placed at 381 mm (15 in), 533 mm (21 in), and 686 mm (27 in) above the ground surface. The ends of the cables were threaded rods that terminated in a cable anchor. Each cable was attached to the impact side of the post utilizing an 8-mm (5/16-in) diameter steel cable-to-post attachment bracket bent into a *J* shape and denoted as a J-bolt, as shown in Figure 2b. The spacing between posts on the curved portion of the system was 2,400 mm (8 ft).

In Test No. NYCC-1, a 2,277-kg (5,020-lb) pickup truck impacted the three-cable barrier system at a speed of 99.1 km/h (61.6 mph) and at an angle of 19.9 degrees (Schmidt, Lechtenberg, et al., 2013). The barrier successfully redirected the vehicle and the test was acceptable according to *MASH* safety performance criteria. The top cable snagged on the front of the vehicle and the threaded cable end fractured 300 ms after the initial impact. For Test No. NYCC-1, the maximum lateral dynamic barrier deflection before the cable release at the end anchorage was 2.6 m (8.5 ft), as determined from high-speed digital video analysis. The maximum

(a)   (b)
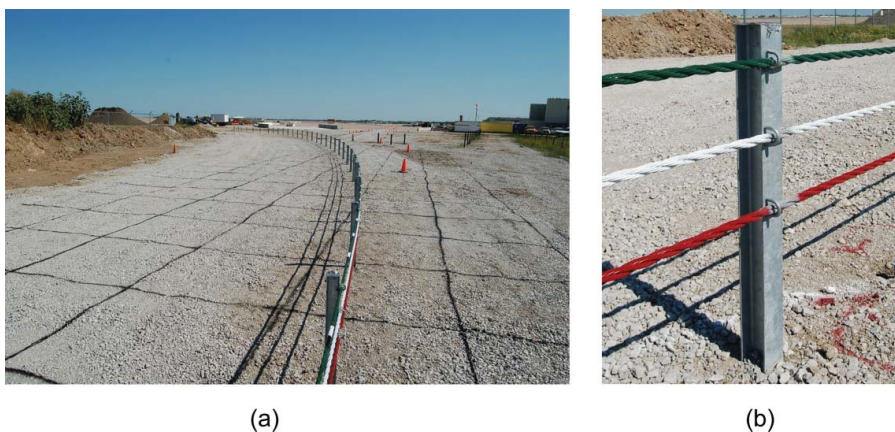
Figure 2. Test installation: (a) exterior-curved cable barrier system; (b) J-bolt.

lateral dynamic barrier deflection after the cable released from the end anchorage was 3.8 m (12 ft – 7 in). The exit velocity of the pickup truck as determined from the accelerometer data analysis was approximately 92.0 km/h (57.2 mph).

In Test No. NYCC-3, the radius of the cable barrier system was increased to 134 m (440 ft), and the cable heights were raised by 51 mm (2 in). All other components and dimensions remained the same as in Test No. NYCC-1. The three-cable barrier system was impacted with a 4,998-lb pickup truck at a speed of 101.6 km/h (63.1 mph) and at an angle of 21.6 degrees (Schmidt, Lechtenberg, et al., 2013). The barrier adequately contained the vehicle, and the test was determined to be acceptable according to the *MASH* safety performance criteria. For Test No. NYCC-3, the maximum lateral dynamic barrier deflection was 3,564 mm (14 ft – 4 in). The velocity of the pickup truck as determined from the accelerometer data analysis was approximately 80.5 km/h (50.0 mph) when the vehicle exited the system. Table 1 summarizes the crash tests impact conditions.

3. Reconstruction technique

In most vehicle-barrier collisions, a portion of the kinetic energy is absorbed by the system through vehicle and barrier crush and deformation. The reconstruction procedure developed is based on conservation of energy derived from examining vehicle and barrier behavior in full-scale crash tests. The summation of the energy absorbed by each energy component during the impact event is equal to the total change in kinetic energy through the impact. These components include the plastic deformation/rotation of posts, tire-ground interaction, internal cable energy, vehicle-barrier interaction, deformation of cable-to-post attachments, and other energies. It is assumed that the velocity of the vehicle when exiting the system was determined through other accident reconstruction techniques (Fricke, 1990). The kinetic energy of the vehicle of known mass ($M_{vehicle}$) when it departs the barrier at a velocity ($V_{departing}$) is calculated using Equation 1. This energy ($KE_{departing}$) is then added to the total energy lost during the impact ($E_{dissipated}$) to estimate the kinetic energy of the vehicle at the initial impact with the guardrail system ($KE_{initial}$) through Equation 2. The initial velocity of the vehicle can then be determined by Equation 3.

$$KE_{departing} = \frac{1}{2}(M_{vehicle})V_{departing}^2 \tag{1}$$

$$KE_{initial} = KE_{departing} + E_{dissipated} \tag{2}$$

$$V_{initial} = \sqrt{\frac{2KE_{initial}}{M_{vehicle}}} \tag{3}$$

Herein, the energy components throughout the barrier impact are quantified, and the proposed methods for estimating the amount of absorbed energy through each component were evaluated using three full-scale crash tests.

The analysis was limited to nonproprietary, low-tension cable barriers. As such, all posts were S3 × 5.7 steel line posts embedded in soil or a concrete foundation, and all cable-to-post attachments were 8-mm (5/16-in) J-bolts. Previous studies pertaining to cable barrier systems and components conducted at the Midwest Roadside Safety Facility (MwRSF) were utilized during the crash investigations. Several full-scale crash tests have been performed on cable barrier systems (Schmidt, Lechtenberg, et al., 2013; Terpsma et al., 2008). In addition, the MwRSF also conducted component tests on S3 × 5.7 posts (Fating, & Reid, 2002; Kuipers & Reid, 2003; Lutting, & Lechtenberg, 2012) and J-bolts (Reid, & Coon, 2002). A finite element analysis of cable wire rope was also used to quantify vehicle to barrier interaction (Reid, Lechtenberg, & Stolle, 2010).

3.1. Plastic deformation/rotation of posts

A plastic hinge is commonly formed at the groundline as cable barrier line posts deform. Kinetic energy is absorbed by plastic flow in the hinge location. The amount of the energy depends on the soil or foundation, post material, the direction of bending (strong or weak axis), and the lateral deflection of the post. Line posts in low-tension, three-cable barrier systems are typically ASTM A36 S3 × 5.7 steel posts with a minimum yield strength of 248 MPa (36 ksi). The material typically has yield strengths varying from 317 MPa to 386 MPa (46 ksi to 56 ksi) depending on the manufacturer. Newer S3 × 5.7 steel posts may be fabricated with ASTM A992 steel with a minimum yield strength of 345 MPa (50 ksi) and typical yield strengths ranging from 345 MPa to 450 MPa (50 ksi to 65 ksi). The energy absorbed by the post will increase when the yield strength of the steel is higher.

In prior research studies, MwRSF conducted dynamic component testing with a bogie vehicle in which force versus lateral deflection was determined for S3 × 5.7 cable line posts at various impact angles. The posts were tested in rigid sleeves at 0-, 60-, 75-, and 90-degree angles (Kuipers & Reid, 2003; Lutting, & Lechtenberg, 2012). The posts were also tested in a compacted, crushed limestone soil material at 0-, 82.5-, and 90-degree angles (Fating, & Reid, 2002; Kuipers, & Reid, 2003). Angles were measured from the direction of a weak-axis impact, that is, the vehicle was assumed to travel parallel to the system.

During a strong-axis post impact, the post will usually twist from a 90-degree orientation after some time. The S3 × 5.7 is often deemed a weak post in highway guardrail systems, which means the post usually deforms before there is much post rotation in soil. Therefore, the energy absorbed by the S3 × 5.7 post in weak-axis impacts is similar in soil and in a rigid sleeve. However, in strong-axis impacts, the post may displace soil. If the posts are installed in soil with no asphalt overlay, the energy absorbed by the posts may be lower as more post rotation occurs rather than plastic deformation. Comparisons of the energy vs. lateral deflection of posts
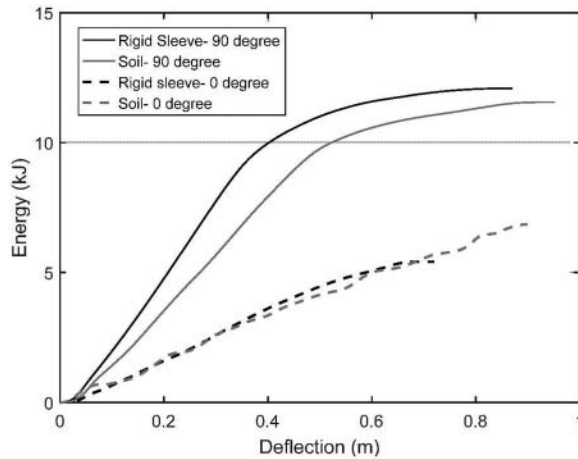
Figure 3. Energy versus deflection – S3 × 5.7 post in soil and rigid sleeve.

embedded in soil and rigid sleeves are shown in Figure 3 for impacts at 0 and 90 degrees. A vehicle impacting at a 0-degree angle (i.e., vehicle parallel to the system) would be more common. At this angle, there is a minimal difference in the energy absorption over 737 mm (29 in) of deflection. For a 90-degree impact angle, the energy absorbed by an S3 × 5.7 post in soil is approximately 25% less than to the same post in a rigid sleeve.

To establish a practical method to estimate the energy absorbed through plastic deformation of the post, the lateral deflection of the post along its impact angle axis would need to be measured, which can be difficult to measure after an impact event. Therefore, the lateral post deflections were converted into deformed heights above the ground by assuming that the posts yield at groundline and the upper part of the post rotates about the hinge point. The energy absorption of the deformed S3 × 5.7 cable post can then be determined by measuring the deformed post height and estimating the deformed post orientation angle. Figure 4 show example charts to determine the energy absorbed based on the deformed post height for the 762-mm (30-in) high S3 × 5.7 posts of a cable barrier system embedded in concrete sleeve and soil, respectively. The angles provided are the orientation of the post after impact from an overhead view (e.g., a 0-degree orientation angle may occur if the vehicle impacts the centerline of the cable barrier posts parallel to the system or roadway). Similarly, charts of the absorbed energy vs deformed post height for posts with different heights are provided in the report by Schmidt, Meyer, et al. (2013).

3.2. Tire-ground interaction

Depending on the site-specific conditions, a vehicle leaving the roadway will encounter a concrete/asphalt paved surface or a grass/soil unpaved surface before impacting a cable barrier system. The energy absorbed by the tire-ground
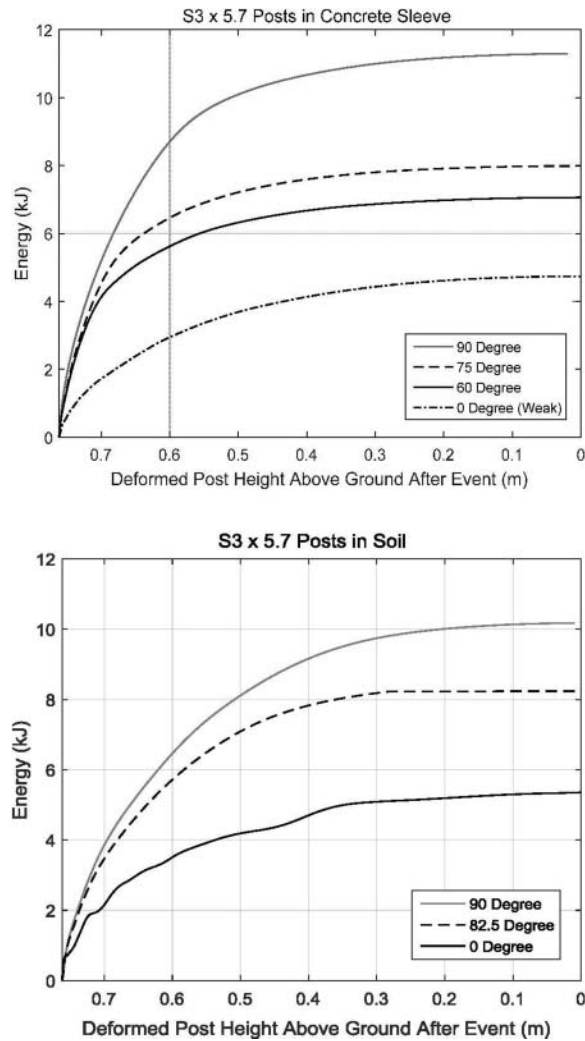
Figure 4. Energy versus deformed post height – S3 × 5.7 post height 30 in.

interaction is approximated multiplying the weight of the vehicle, the distance travelled, and the coefficient of rolling resistance or drag factor between the vehicle and ground. The distance travelled by the vehicle from initial barrier impact to exit should be measured, and the vehicle trajectory marks need to be studied to determine when the vehicle tires were rolling, sliding, and/or braking. For the purposes of this study, it was assumed that the vehicle did not rollover and remained upright on all tires. When the vehicle is tracking (i.e., tires rolling normally), the coefficient of rolling resistance is small and varies slightly with the road surface. Most of the time, when a vehicle leaves the roadway, driver will be actively braking, which creates a high drag factor between the skidding tires and the ground surface adjacent to the barrier system. This drag factor is significant, but it is not easy to quantify. Once the vehicle impacts a cable barrier system, the vehicle may transition between

tracking and nontracking (i.e., tires sliding laterally) conditions. Tire-ground coefficients for various road/ground surfaces and for different braking/skidding and rolling scenarios are provided in various sources, including Trantham (2009). These values were used to estimate the total kinetic energy lost through tire-ground interaction during the full-scale crash tests.

3.3. Internal cable energy

The tension in cables increases as a vehicle deflects the cable barrier system during an impact event. The energy due to the cables transferred to the barrier is equal to the integral of the lateral force component of the cable tension applied to the vehicle over the lateral deflection of the barrier, as shown in Equation 4. Note the lateral force component of the cable tension refers to the projection of the cable tension along the lateral direction as the vehicle deforms the cable. The dynamic cable tension during an impact varies between straight, exterior-curved, and interior-curved cable barrier systems. The energy absorbed during an impact event with a straight system and an exterior-curved system was analyzed in two full-scale crash tests, Test No. CS-2 (Terpsma et al., 2008) and Test No. NYCC-3 (Schmidt, Lechtenberg, et al., 2013). Full-scale crash testing of an interior-curved system was not available. The lateral redirective cable force (F_{Lat}) was estimated in full-scale crash tests based on the measured tension (T) as well as the leading and trailing angles (θ_1 and θ_2) measured from high-speed film that were formed by the cable in contact with the vehicle, as shown in Figure 5, using Equation 4.

$$F_{Lat} = T(\sin\theta_1 + \sin\theta_2) \tag{4}$$

The angles vary as the vehicle initially impacts the barrier, becomes parallel to the system, and then redirects away from the barrier. The leading and trailing angles, the lateral displacement of the vehicle, and the total distance travelled were measured from overhead video using AutoCAD at 30-ms or 50-ms discrete time intervals. The energy absorbed as a function of the lateral wheel trajectory can be found by integrating the lateral force versus lateral wheel trajectory curve, as
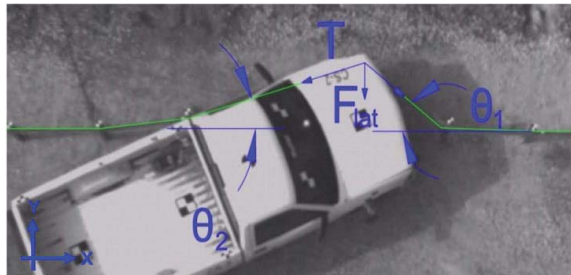

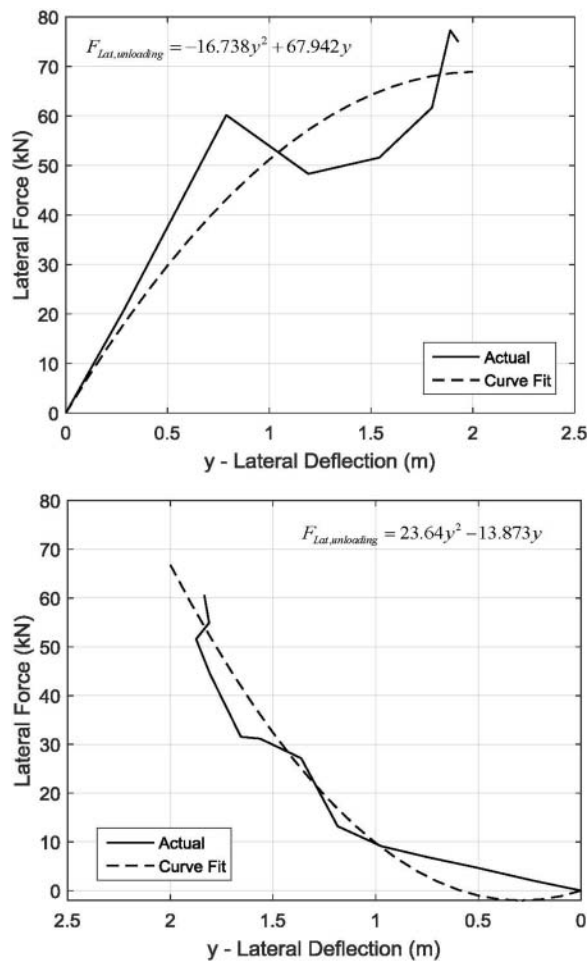**Figure 5.** Parameters associated with cable contact with vehicle.

Figure 6. Lateral cable force versus lateral deflection of straight cable barrier system (a) during loading and (b) during unloading.

shown in Equation 4. The vehicle's kinetic energy due to internal cable energy decreases during loading and then increases during unloading. The change in energy between these two curves represents the internal cable energy loss. Relationships between the lateral force and the lateral wheel trajectory were found for Test Nos. CS-2 and NYCC-3. Additional full-scale crash testing of cable barrier systems is necessary to determine if the relationships apply to systems with different post spacing, system lengths, curve radii, and impact conditions.

For the straight cable barrier system in Test No. CS-2, the lateral cable force was calculated from the tension and cable angles during cable loading and unloading, as shown in Figure 6. The actual curves in Figure 6 were integrated, and the change in the energy was calculated to be 41.5 kJ (30.6 kip-ft), which represents the internal cable energy lost during the impact event. In a roadside crash accident, cable tension, leading and trailing angles, and system deflections throughout the impact would not be known. However, curves were

fitted to the data and were integrated with respect to the lateral deflection (y), (Equation 5). Relations to estimate the energies during loading and unloading with respect to the maximum lateral deflection (y_{max}) are provided in Equations 6 and 7.

$$E_{loading} = \int_0^{y_{max}} F_{lat,loading} \, dy \tag{5}$$

$$E_{Loading} = -5.578 y_{max}^3 + 33.97 y_{max}^2 \tag{6}$$

$$E_{Unloading} = 7.88 y_{max}^3 - 6.93 y_{max}^2 \tag{7}$$

For the exterior curved cable barrier in Test No. NYCC-3, the lateral cable force was calculated from the tension and cable angles during cable loading and cable unloading, shown in Figure 7. The actual curves in Figure 7 were integrated, and
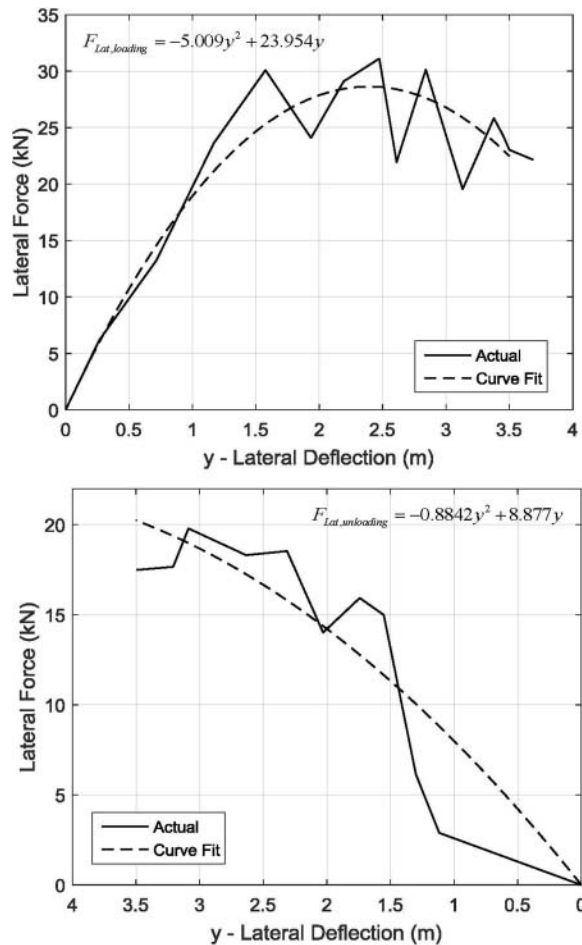

Figure 7. Lateral cable force versus lateral deflection of exterior-curved cable barrier system (a) during loading and (b) during unloading.

the change in the energy was calculated to be 48.4 kJ (35.7 kip-ft), which represents the internal cable energy lost during the impact event. Similar to the straight cable system, the fitted curves were integrated with respect to the lateral deflection (y), and relations to estimate the energies during loading and unloading with respect to the maximum lateral deflection (y_{max}) are provided in Eqations 8 and 9.

$$E_{Loading} = -1.6696y_{max}^{3} + 11.977y_{max}^{2} \tag{8}$$

$$E_{Unloading} = -0.2947y_{max}^{3} + 4.4385y_{max}^{2} \tag{9}$$

3.4. Vehicle-barrier frictional interaction

The energy absorbed due to the vehicle-barrier friction is equal to the integral of the lateral cable force over the total distance multiplied by the coefficient of friction between the vehicle and barrier over the distance the vehicle travelled. Previous computer simulation of cable barrier system impacts has shown that a coefficient of friction of 0.08 has been used in validated cable barrier system models (Reid et al., 2010). Therefore, the vehicle-barrier coefficient of friction was estimated to be in the range from 0.08 to 0.12. The upper range may be applicable when there is very apparent vehicle damage due to cables sliding along the sheet metal. However, no physical testing data was known between cables and sheet metal. Thus, a larger range of coefficients may be used for a conservative approach during accident reconstructions. The upper and lower bounds of vehicle-barrier frictional energy using coefficients of 0.08 and 0.12 vs. the total distance travelled were found for a straight cable system (Test No. CS-2) and an exterior-curved cable system (Test No. NYCC-3), as shown in Figure 8. Additional full-scale crash testing of cable barrier systems is necessary to determine if the relationships apply to systems with different post spacing, system lengths, curve radii, and impact conditions.
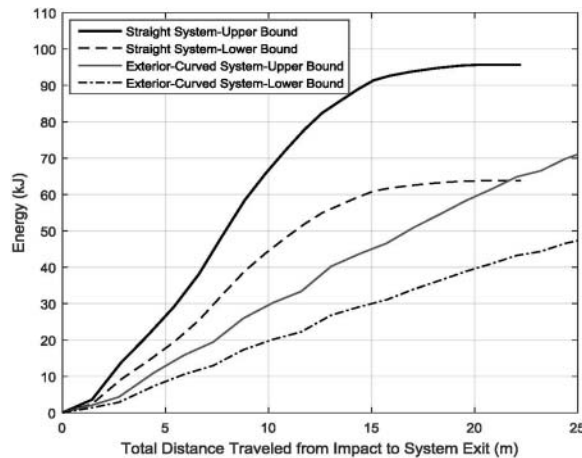

Figure 8. Vehicle-barrier frictional energy versus total distance travelled.
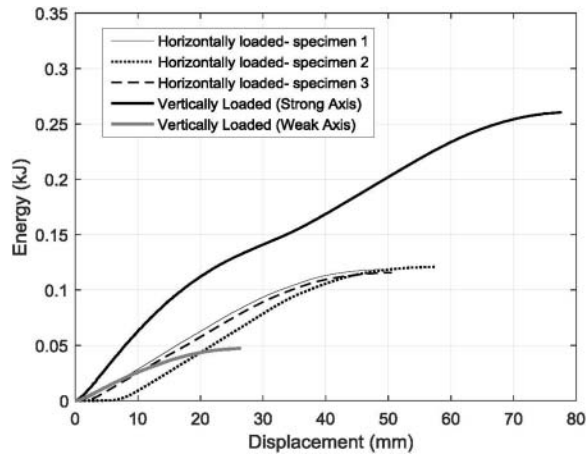
Figure 9. Energy versus displacement – cable-post attachment (Reid, & Coon, 2002).

3.5. Cable-post attachment deformation

The energy absorbed through the deformation of the 8-mm (5/16-in) J-bolts, which retain the cables to the posts, was investigated. MwRSF completed a component testing program in which 8-mm (5/16-in) J-bolts were loaded vertically and horizontally (Reid, & Coon, 2002). A simulated cable, which was a 19-mm (3/4-in) diameter steel bar, was mounted in a material testing systems (MTS) machine to load the J-bolts in three configurations: (1) a vertical load to simulate a cable pulling the J-bolt upward, (2) a vertical load to simulate a cable pulling the J-bolt downward, and (3) a horizontal load to simulate a cable pulling the J-bolt away from a post.

The energy versus displacement curves for each of the 8-mm (5/16-in) J-bolt loading cases are shown in Figure 9. For the upward, downward and horizontal load configurations, the total energy absorbed through the J-bolt deformation was 0.047, 0.258, and 0.122 kJ (0.035, 0.19, and 0.09 kip-ft, respectively). The greatest energy dissipation occurred when the J-bolt was loaded vertically downward. If all three cables on a single post were pulled downward, 0.773 kJ (0.57 kip-ft) of energy would be dissipated. However, the cables commonly release from the posts during an impact in the upward or horizontal direction, so the energy due to J-bolt deformation is likely to be much smaller than 0.773 kJ (0.57 kip-ft) per post. Therefore, the energy dissipated by the J-bolts was considered negligible and was not included in the calculation of the total energy dissipated in the full-scale test analyses.

4. Reconstruction technique validation

The reconstruction technique was implemented for three full-scale crash tests on straight and curved, low-tension cable barrier systems. Test No. CS-2, which was conducted with a pickup truck impacting a straight three-cable barrier system, was used to detail the steps of the reconstruction procedure. The exit velocity of the

pickup truck was approximately 52.8 km/h (32.8 mph). The known kinetic energy of the pickup truck at impact and at exit was approximately 770.4 kJ (568.2 kip-ft) and 218.8 kJ (161.3 kip-ft), respectively. Therefore, 551.6 kJ (406.9 kip-ft) of energy was absorbed during the impact.

In Test No. CS-2, 18 posts, fabricated from ASTM A36 steel, plastically deformed during the impact. The posts had an initial height of 838 mm (33 in) and were installed in soil. The energy absorbed by each post was estimated from charts provided by Schmidt, Meyer, et al. (2013). The weight of the vehicle without any occupants was 2,033 kg (4,481 lb). The vehicle trajectory was used to determine when the vehicle was tracking (i.e., rolling on all wheels) and when it was nontracking (i.e., sliding) and the distance of each tracking and nontracking event for each wheel. During the times when the tires were rolling, the tire-ground coefficient range was 0.01 to 0.0375 for new, sharp concrete to sandy dirt, as determined from Trantham (2009). During the times when the vehicle was sliding or nontracking, the tire-ground coefficient range was 0.4 to 0.7 for dry loose gravel at a velocity greater than 48 km/h (30 mph). The estimated energy absorbed by the tire-ground interaction ranged from 135.3 kJ to 238.9 kJ (99.8 kip-ft to 176.2 kip-ft).

The maximum lateral deflection of the vehicle in the system was found to be 1.9 m (6.3 ft). The difference between the energies at maximum lateral deflection was the energy absorbed by the cables using Equations 6 and 7 was approximately 47.4 kJ (35.0 kip-ft). Friction occurred between the vehicle and the cables due to the lateral cable loading. The coefficient of friction between the vehicle and cables ranged from 0.08 to 0.12, and the total distance travelled was 22.25 m (73 ft). Thus, the total energy absorbed by the vehicle-barrier friction from Figure 8 ranged from 63.8 kJ to 95.7 kJ (47.1 kip-ft to 70.6 kip-ft). The energy of all components is summarized in Table 2. The known kinetic energy of the vehicle when it exited the system was 218.8 kJ (161.3 kip-ft). The vehicle's estimated initial velocity was 88.7 km/h ± 4.9 km/h (55.1 mph ± 3.0 mph). The actual velocity of the vehicle was 99.1 km/h (61.6 mph), which is higher than the reconstruction technique predicted range. This potentially could be due to the other energy components that were unaccounted for, underestimated coefficients of tire-ground and vehicle-barrier interaction, contributions of the sloped soil region behind the barrier, or inaccuracies in estimating deformed post height and orientations.

The same procedure was repeated for Test Nos. NYCC-1 and NYCC-3, where the exterior-curved cable barriers were impacted by a pickup truck, and the determination of each energy component was summarized by Schmidt, Meyer, et al. (2013), as shown in Table 2. The actual impact speeds with the exterior-curved cable barriers were within the ranges of the reconstructed impact speeds. The results of the three reconstruction cases studied are shown in Table 3.

As an example, a view of Test No. NYCC-3 is shown in Figure 10 to illustrate how the required measurements including maximum lateral deflection and total travelled distance can be obtained from the crash scene.

Table 2. Summary of energy components.

Test No. CS-2					
Actual Initial Energy (kJ)			770.4		
Actual Exit Energy (kJ)			218.8		
Actual Initial Velocity (km/h)			99.1		
Actual Exit Velocity (km/h)			52.8		
	Lower Bound (kJ)	Total %	Upper Bound (kJ)	Total %	
Posts	86.0	26	86.0	18	
Tire-Ground	135.3	41	238.9	51	
Cable Redirection	47.5	14	47.5	10	
Vehicle-Barrier	63.9	19	95.7	20	
Total Energy (kJ)	332.4		468.0		
Estimated Initial Velocity (km/h)	83.84		93.5		
Test No. NYCC-1					
Actual Initial Energy (kJ)			862.9		
Actual Exit Energy (kJ)			743.2		
Actual Initial Velocity (km/h)			99.1		
Actual Exit Velocity (km/h)			92.0		
	Lower Bound (kJ)	Total %	Upper Bound (kJ)	Total %	
Posts	24.5	30	24.5	26	
Tire-Ground	1.9	2	7.1	8	
Cable Redirection	41.6	51	41.6	45	
Vehicle-Barrier	13.4	17	20.2	22	
Total Energy (kJ)	81.5		93.3		
Estimated Initial Velocity (km/h)	96.88		97.5		
Test No. NYCC-3					
Actual Initial Energy (kJ)			850.5		
Actual Exit Energy (kJ)			540.2		
Actual Initial Velocity (km/h)			101.6		
Actual Exit Velocity (km/h)			80.5		
	Lower Bound (kJ)	Total %	Upper Bound (kJ)	Total %	
Posts	64.4	23	64.4	16	
Tire-Ground	118.9	42	217.7	53	
Cable Redirection	43.8	15	43.8	11	
Vehicle-Barrier	56.0	20	84.1	20	
Total Energy (kJ)	283.1		410.0		
Estimated Initial Velocity (km/h)	97		104.3		

5. Summary of reconstruction procedure

To reconstruct a low-tension, three-cable barrier system impact, the mass of vehicle, initial height of posts, and foundation of posts (whether soil or concrete sleeve) must be known. A summary of the procedure to reconstruct the initial velocity of vehicle when it impacts a cable barrier is as follows:

1. The velocity of the vehicle as it exits the barrier must be determined through conventional accident reconstruction techniques (Fricke, 1990). Then the departing kinetic energy of the vehicle is calculated using Equation 1.

Table 3. Comparison of reconstruction results to actual crash test data.

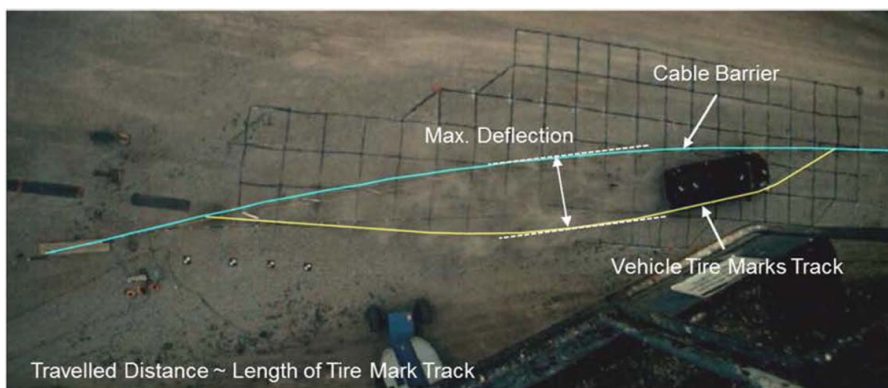| Test No.	Cable Barrier System	Reconstructed Speed (km/h)	Actual Speed (km/h)	Difference (%)
CS-2	Straight	88.7 ± 4.9	99.1	−10.5
NYCC-1	Exterior-curved	98.1 ± 0.4	99.1	−1.0
NYCC-3	Exterior-curved	100.6 ± 3.7	101.6	−0.98

Figure 10. Postcrash overhead view — Test No. NYCC.

2. The energy absorbed by the plastic deformation and rotation of posts embedded in ground is calculated. This is determined from Figure 4 for 762 mm (30-in) tall posts or from charts provided in report by Schmidt, Meyer, et al. (2013). Based on the type of the post foundation (either soil or concrete sleeve) and the initial height of the posts (ranging from 711 mm to 838 mm), the charts give the energy absorbed by deformation and rotation of the posts versus the deformed post height above ground after impact. This method is not applicable to posts that do not form a plastic hinge, such as posts with a slip base.

3. The energy absorbed by the tire-ground interaction is approximated by multiplying the weight of the vehicle by the coefficient of rolling resistance or drag factor between the vehicle and ground and the distance travelled. The vehicle trajectory marks should be evaluated for each wheel to determine the configuration of the tire throughout the impact event. Vehicle-ground coefficients for various road/ground surfaces and for different braking/skidding and rolling scenarios can be found in various sources, including Trantham (2009).

4. The internal cable energy can be estimated by measuring the maximum lateral deflection of the barrier based on vehicle trajectory marks. The energy absorbed up to maximum deflection during loading and then after maximum deflection during unloading is calculated through Equations 6 through 9 (Equations 6 and 7 for straight cable system and Equations 8 and 9 established for curved cable barrier system). The difference between the loading and unloading energies represents the internal cable energy lost during the impact event.

5. The energy absorbed due to the vehicle-barrier friction using a coefficient of friction ranging from 0.08 to 0.12 is also found using Figure 8 as a function of the distance that the vehicle travelled from impact to exit. The total distance travelled can be determined from vehicle trajectory marks.

6. The departing kinetic energy is added to the total energy calculated in Steps 2 through 5 to estimate the initial kinetic energy of the vehicle impacting the cable barrier system using Equation 2.

7. Lastly, the initial velocity of the vehicle can then be determined by Equation 3.

6. Conclusions and recommendations

A procedure was developed to estimate initial vehicle velocity for cable-barrier impacts. This method includes a series of charts recommended based on full-scale crash tests as well as component tests. The energy absorbed during a cable barrier impact was divided into several components: (1) plastic deformation/rotation of posts, (2) tire-ground interaction, (3) internal cable energy, (4) vehicle-barrier frictional interaction, and (5) cable-post attachments (J-bolt) deformation. The energy absorbed by deforming the J-bolt cable clips was analyzed and determined to be negligible. The kinetic energy upon exiting the barrier system added to the calculated total energy lost during the impact provided an estimate of the kinetic energy and velocity of the vehicle at the initial barrier impact. This technique was validated using three full-scale crash tests. The reconstructed velocities were 1 to 10% within the actual values. However, additional analysis on curved and straight barrier systems is recommended to determine if the relationships apply to systems with different post spacing, system lengths, curve radii, and impact conditions.

In the proposed crash reconstruction technique, the kinetic energy upon exiting the barrier system added to the calculated total energy lost during the impact provided an estimate of the kinetic energy and velocity of the vehicle at the initial barrier impact. The total energy lost during the impact was obtained from the components which are not dependent on either the impacting vehicle or the cable barrier type (e.g., 4-cable barrier). However, the impact height may be slightly different for different vehicles that potentially affects the results and needs to be considered. Note that the friction coefficients between vehicle and barriers are fairly similar for different vehicle type. Thus, it might be reasonable to carefully apply the proposed crash reconstruction method for similar cable barriers (e.g., 4-cable barrier) and for different vehicles (e.g., small passenger car). However, additional research and testing is required to confirm the validity of this method for other crash scenarios.

ORCID

Mojdeh Asadollahi Pajouh   http://orcid.org/0000-0002-4906-8562

References

American Association of State Highway and Transportation Officials. (2009). *Manual for assessing safety hardware (MASH)*. Washington, DC: American Association of State Highway and Transportation Officials.

Coon, B. A., & Reid, J. D. (2005). Crash reconstruction technique for longitudinal barriers. *Journal of Transportation Engineering, 131*(1), 54–62. doi:10.1061/(ASCE)0733-947X(2005)131:1(54).

Coon, B. A., & Reid, J. D. (2006). Reconstruction techniques for energy-absorbing guardrail end terminals. *Accident Analysis and Prevention*, *38*(1), 1–13. doi:10.1016/j.aap.2005.06.016.

Fating, R. M., & Reid, J. D. (2002). *Dynamic impact testing of S75x8.5 steel posts (cable barrier posts)* (Report No. TRP-03-117-02). Lincoln, NE: University of Nebraska-Lincoln, Midwest Roadside Safety Facility.

Fricke, L. B. (1990). Traffic accident reconstruction: Traffic accident investigation manual (Vol. 2). Evanston, IL: Northwestern University Press.

Kuipers, B. D., & Reid, J. D. (2003). *Testing of M203x9.7 (M8x6.5) and S76x8.5 (S3x5.7) steel posts – Post comparison study for the cable median barrier* (Report No. TRP-03-143-03). Lincoln, NE: University of Nebraska-Lincoln, Midwest Roadside Safety Facility.

Lutting, M., & Lechtenberg, K. A. (2012). *Cut cable post bogie testing test nos. CCP-1 through CCP-11* (Internal Report). Lincoln, NE: University of Nebraska-Lincoln, Midwest Roadside Safety Facility.

Mak, K. K., & Sicking, D. L. (1990). *Rollover caused by concrete safety-shaped barriers*. Transportation Research Record No. 1258. Washington, DC: Transportation Research Board, National Academy Press.

Powell, G. H. (1973). *BARRIER VII: A computer program for evaluation of automobile barrier systems* (Report No. FHWA-RD-73-51). Washington, DC: Federal Highway Administration.

Reid, J. D., & Coon, B. A. (2002). *Finite element modeling of cable hook bolts* (7th Ed.). Dearborn, MI: International LS-DYNA Users Conference, Simulation 2002.

Reid, J. D., Lechtenberg, K. A., & Stolle, C. S. (2010). *Development of advanced finite element material models for cable barrier wire rope* (MATC-UNL Report No. 220, MwRSF Research Report No. TRP-03-233-10). Lincoln, NE: University of Nebraska-Lincoln, Midwest Roadside Safety Facility.

Ross, H. E., Sicking, D. L., Zimmer, R. A., & Michie, J. D. (1993). *NCHRP Rep. 350: Recommended procedures for the safety performance evaluation of highway features*. Washington, DC: National Research Council, National Cooperative Research Program.

Schmidt, J., Meyer, C. L., Lechtenberg, K. A., Faller, R. K., Bielenberg, R. W., & Reid, J. D. (2013). *Energy analysis of vehicle-to-cable barrier impacts* (Report No. TRP-03-283-13). Lincoln, NE: University of Nebraska-Lincoln, Midwest Roadside Safety Facility..

Schmidt, T. L., Lechtenberg, K. A., Meyer, C. L., Faller, R. K., Bielenberg, R. W., & Reid, J. D. (2013). *Evaluation of the New York low-tension curved three-cable barrier* (Report No. TRP-03-263-12). Lincoln, NE: University of Nebraska-Lincoln, Midwest Roadside Safety Facility.

Terpsma, R. J., Polivka, K. A., Sicking, D. L., Rohde, J. R., Reid, J. D., & Faller, R. K. (2008). *Evaluation of a modified three cable guardrail adjacent to steep slope* (Report No. TRP-03-192-08). Lincoln, NE: University of Nebraska-Lincoln, Midwest Roadside Safety Facility.

Trantham, N. (2009). *Post impact drag factor. Technical accident investigation*. Lincoln, NE: Law Enforcement Training Center.